

# Effect of quadric shear basic zonal flows and topography on baroclinic instability

By XIUJIE ZHANG, HONGXIN ZHANG, YUYING YANG, and JIAN SONG\*,  
*College of Sciences, Inner Mongolia University of Technology, Hohhot, China*

(Manuscript Received 16 March 2020; in final form 22 October 2020)

## ABSTRACT

On the  $\beta$  plane approximation, the two-layer quasigeostrophic mode is used to study the baroclinic instability of the quadric shear basic zonal flows on a uniform bottom topography. The phase speed and growth rate of instability waves are functions of the shear zonal basic flows and bottom topographic slope. The study focus is on the effects of topography and the quadric shear basic zonal flows (the second derivative of basic zonal flows is not zero). The meridional slope destabilise (stabilise) zonal flows, it plays an unstable role in disturbance, moreover the effect of the second derivative of basic zonal flows is to accelerate the instability of disturbance. The zonal slope always destabilises the zonal basic flows through zonal and meridional wavenumber. Moreover, the effect of the second derivative of basic zonal flows is to accelerate the instability of disturbance.

*Keywords: topographic slope, basic zonal flows, quadric shear, baroclinic instability,  $\beta$  plane approximation*

## 1. Introduction

Baroclinic instability of oceanic currents could yield the right orders of magnitude of the properties of the Gulf Stream eddies. In a macroscale background current the original condition of eddy development is depicted through the rapid growth of infinitely small orthogonal mode perturbations, which can, owing to their spatial and time structure, efficiently obtain energy from the large-scale background state (Pedlosky, 1978; Cushman-Roisin, 1986). The physical mechanism of eddy generation depends on the mean potential vorticity (PV) gradient, which is prerequisites large-scale flows for unstable and nonlinear evolution of eddy flows. Although the planetary vorticity gradient  $\beta$  is small, the nonlinear dynamics of the instability waves very susceptible to the  $\beta$  effect as has been proved in an earlier research, it is further found that the  $\beta$  effect inclines to preserve the instability point at the primary of the solution phase plane from the solution trajectories (Pedlosky, 1981). Chaney (1974) and Eady (1949) formulated a model baroclinic instability, they indicated that the disturbance viewed in the atmosphere and ocean could be interpreted as a manifestation of baroclinic instability of the basic zonal flows. A simple two-layer model with small vertical

scale to remove interference was first introduced by Phillips (1954). Pedlosky (1987) used Phillips' model to study nonzonal basic flows with a flat bottom topography, he showed that the nonzonal basic flows would not possess a minimum critical shear for instability. More recently, Pedlosky studied the evolution of baroclinic instability wave in spatial and time structure, when the disturbance shifts downstream from an upstream source of perturbation energy such as might take place in flows like the separated Gulf Stream (Pedlosky, 2011, 2019).

A central question in the theory of atmosphere and ocean instability barotropic and baroclinic modes are modified by the presence of the basic flows shear or variable topography. The influence of bottom topography on large-scale atmospheric and oceanic flows have formed the theme for a large number of meteorological and ocean station investigations. The bottom topography were studied by many researchers (Rhines and Bretherton, 1973; McWilliams, 1974; Patoine and Warn, 1982), who demonstrate that it can strongly adapt to the dynamics of waves in the ocean, the role of bottom slope is similar to the  $\beta$  effect, which generally assists stabilise the zonal basic flows by modifying the background PV gradient (Blumsack and Gierasch, 1972; Steinsaltz, 1987). Hart demonstrated that a one-way zonal slope has an equilibrium effect on a circular vortex and forms an asymmetric mean flows in a two-layer quasigeostrophic

\*Corresponding author. e-mail: Jian Song  
songjian@imut.edu.cn

(QG) model on  $f$  plane (Hart, 1975a, 1975b). Benilov has shown that short-scale bottom topography irregularities can stabilise the current (Benilov, 2001). On the  $\beta$  plane approximation, Chen and Kamenkovich (2013) used a two-layer QG model, they obtained the important effect of bottom topography on the baroclinic instability of basic zonal currents. They found the topographic slope powerful affects the instability scale, showing that a positive topographic slope can lead to a large scale of most instability wave, whilst a negative topographic slope is easy to make the wave with the maximum growth rate changes a smaller scale. Many studies only consider the influence of zonal basic flows or nonzonal basic flows and topography on baroclinic instability, in addition, the deviation of most instability is litter consideration on the combined effect of the quadric shear basic zonal flows and topographic slope on the  $\beta$  plane approximation (Leng and Bai, 2018).

In this study, the quadric shear basic zonal flows and bottom slope were considered on the  $\beta$  plane approximation, to examine it and the topography effects on the linear baroclinic instability. This paper is organised as follows: a two-layer model of the quadric shear basic zonal flows is described in Section 2; Under the quadric shear basic zonal flows, a necessary instability condition and the dispersion relation for instability model are derived and the second derivative of basic zonal flows, topographic slope effects are discussed in Section 3. In Section 4, Conclusions are drawn in section.

## 2. The model

A two-layer potential vorticity (PV) equation with topography on the  $\beta$  plane approximation (Geoffrey and Vallis, 2006)

$$\frac{\partial q_n}{\partial t} + J(\psi_n, q_n) = 0 \quad (n = 1, 2), \quad (1)$$

where  $q_n$  is potential vorticity, the subscript refers to the layer; the upper layer corresponds to  $n = 1$ , and the lower to  $n = 2$ .  $J(a, b) = \frac{\partial a}{\partial x} \frac{\partial b}{\partial y} - \frac{\partial a}{\partial y} \frac{\partial b}{\partial x}$  is the Jacobian operator. Potential vorticity  $q_n$  are of the form on the  $\beta$  plane approximation

$$q_n = \nabla^2 \psi_n + (-1)^n F_n (\psi_1 - \psi_2) + \beta y + \delta_{n2} \frac{f_0}{H_n} \eta_b(x, y). \quad (2)$$

where  $\beta$  is the planetary vorticity gradient,  $H_n$  is the depth of two-layer fluid,  $\eta_b(x, y)$  is the spatially varying elevation of bottom topography,  $F_n = \frac{f_0^2}{g' H_n}$ , square of the inverse Rossby radius,  $f_0$  is the Coriolis parameter,  $g'$  is the reduced gravity,  $\delta_{n2}$  is the Kronecker symbol,

$$\delta_{n2} = \begin{cases} 0, & n \neq 2, \\ 1, & n = 2. \end{cases}$$

Consider the streamfunction  $\psi_n$  in the upper layer and lower layer:

$$\psi_n = \Psi_n(y) + \varphi_n, \quad (3)$$

where  $\varphi_n$  describe disturbances,  $U_n(y) = -\frac{d\Psi_n}{dy}$  is the quadric shear basic zonal flows ( $\frac{d^2 U_n}{dy^2} \neq 0$ ) in the upper layer. The potential vorticity  $q_n$  is expressed through the streamfunction  $\psi_n$  as follows:

$$q_1 = \nabla^2 \varphi_1 - \alpha_1 F (\varphi_1 - \varphi_2 + \Psi_1(y) - \Psi_2(y)) + \beta y - \frac{dU_1}{dy}, \quad (4)$$

$$q_2 = \nabla^2 \varphi_2 + \alpha_2 F (\varphi_1 - \varphi_2 + \Psi_1(y) - \Psi_2(y)) + \beta y - \frac{dU_2}{dy} + \frac{f_0}{H_2} \eta_b(x, y), \quad (5)$$

We define

$$F = \frac{f_0^2 (H_1 + H_2)}{g' H_1 H_2},$$

For convenience, let

$$\alpha_1 = \frac{H_2}{(H_1 + H_2)}, \quad \alpha_2 = \frac{H_1}{(H_1 + H_2)}.$$

The square of the inverse Rossby radius  $F_n$  follows that

$$F_1 = \alpha_1 F, \quad F_2 = \alpha_2 F. \quad (6)$$

## 3. Instability analytical study

### 3.1. Necessary instability condition with quadric shear basic zonal flows and bottom topography

The perturbation equations for  $\varphi_n$  are obtained by linearising the PV equation (1):

$$\begin{aligned} & \left( \frac{\partial}{\partial t} + U_1 \frac{\partial}{\partial x} \right) [\nabla^2 \varphi_1 - \alpha_1 F (\varphi_1 - \varphi_2)] \\ & + \left( \beta - \frac{d^2 U_1}{dy^2} + \alpha_1 F (U_1 - U_2) \right) \frac{\partial \varphi_1}{\partial x} \\ & = 0, \end{aligned} \quad (7)$$

$$\begin{aligned} & \left( \frac{\partial}{\partial t} + U_2 \frac{\partial}{\partial x} \right) [\nabla^2 \varphi_2 + \alpha_2 F (\varphi_1 - \varphi_2)] \\ & + \left( \beta - \frac{d^2 U_2}{dy^2} - \alpha_2 F (U_1 - U_2) + S_y \right) \frac{\partial \varphi_2}{\partial x} - S_x \frac{\partial \varphi_2}{\partial y} \\ & = 0. \end{aligned} \quad (8)$$

where  $S_x = \frac{s_y f_0}{H_2} = \frac{f_0}{H_2} \frac{\partial \eta_b}{\partial x}$ ,  $S_y = \frac{s_x f_0}{H_2} = \frac{f_0}{H_2} \frac{\partial \eta_b}{\partial y}$ ,  $s_x$  and  $s_y$  are the same as employed in Chen and Kamenkovich (2013). The normal-mode solution

$$\varphi_n = A_n e^{i(kx+ly-\omega t)}, \quad (9)$$

where  $A_n$  is the amplitude in each layer,  $(k, l)$  is the wave-number, and  $\omega$  is the frequency of the disturbance. Inserting Eq. (9) into Eqs. (7) and (8) leads to two coupled algebraic equations for  $A_n$ :

$$\left[ (\omega - U_1 k)(K^2 + \alpha_1 F) + k \left( \beta - \frac{d^2 U_1}{dy^2} + \alpha_1 F U_s \right) \right] A_1 - (\omega - U_1 k) \alpha_1 F A_2 = 0, \quad (10)$$

$$(\omega - U_2 k) \alpha_2 F A_1 - \left[ (\omega - U_2 k)(K^2 + \alpha_2 F) + k \left( \beta - \frac{d^2 U_2}{dy^2} - \alpha_2 F U_s \right) + \kappa \right] A_2 = 0, \quad (11)$$

where  $K^2 = k^2 + l^2$ ,  $U_s = U_1 - U_2$ , it represents the vertical shear of the basic zonal flow,  $\kappa = \frac{f_0}{H_2} (\mathbf{K} \times \nabla \eta_b) = \frac{f_0}{H_2} \left( k \frac{\partial \eta_b}{\partial y} - l \frac{\partial \eta_b}{\partial x} \right)$ ,  $\mathbf{K} = (k, l)$  and  $\nabla \eta_b$  are the wave vector and topographic slope, respectively. For obtain a necessary instability condition. Multiplying Eqs. (10) and (11) by  $\frac{\alpha_2 F A_1^*}{U_1 - c}$  and  $\frac{\alpha_1 F A_2^*}{U_2 - c}$ , respectively.

$$\alpha_2 F K^2 |A_1|^2 + \alpha_1 \alpha_2 F^2 (|A_1|^2 - A_1^* A_2) - \frac{\alpha_2 F |A_1|^2 \left( \beta - \frac{d^2 U_1}{dy^2} + \alpha_1 F U_s \right)}{U_1 - c} = 0, \quad (12)$$

$$\alpha_1 F K^2 |A_2|^2 + \alpha_1 \alpha_2 F^2 (|A_2|^2 - A_1 A_2^*) - \frac{\alpha_1 F |A_2|^2 \left( \beta - \frac{d^2 U_2}{dy^2} - \alpha_2 F U_s + \frac{\kappa}{k} \right)}{U_2 - c} = 0. \quad (13)$$

where  $c = \frac{\omega}{k}$  is phase speed,  $A_n^*$  are the complex conjugates of  $A_n$ . Summing up Eqs. (12) and (13), we obtain

$$K^2 F (\alpha_2 |A_1|^2 + \alpha_2 |A_2|^2) + \alpha_1 \alpha_2 F^2 [|A_1|^2 + |A_2|^2 - (A_1^* A_2 + A_1 A_2^*)] - \frac{\alpha_2 F |A_1|^2 \left( \beta - \frac{d^2 U_1}{dy^2} + \alpha_1 F U_s \right)}{U_1 - c} - \frac{\alpha_1 F |A_2|^2 \left( \beta - \frac{d^2 U_2}{dy^2} - \alpha_2 F U_s + \frac{\kappa}{k} \right)}{U_2 - c} = 0. \quad (14)$$

The imaginary part of Eq. (14)

$$\left[ \frac{\alpha_2 F |A_1|^2}{|U_1 - c|^2} \left( \beta - \frac{d^2 U_1}{dy^2} + \alpha_1 F U_s \right) \right]$$

$$+ \frac{\alpha_1 F |A_2|^2}{|U_2 - c|^2} \left( \beta - \frac{d^2 U_2}{dy^2} - \alpha_2 F U_s + \frac{\kappa}{k} \right) \omega_i = 0, \quad (15)$$

where  $\omega_i$  is the imaginary part of  $\omega$ . If  $k$  is not zero, the instability necessary conditions with the basic zonal flows quadric sheared and bottom topography on the  $\beta$  plane approximation.

$$\left( U_s + \frac{\beta - \frac{d^2 U_1}{dy^2}}{\alpha_1 F} \right) \left( U_s - \frac{\beta - \frac{d^2 U_2}{dy^2} + \frac{\kappa}{k}}{\alpha_2 F} \right) > 0. \quad (16)$$

Equation (16) is the ordinary result, it consists of some special cases.

*Case one:* If  $\frac{d^2 U_n}{dy^2} = 0$ , namely the basic zonal flows  $U_n$  is not the quadric shear, the instability necessary conditions,  $\min\left(-\frac{\beta}{\alpha_1 F}, \frac{\beta + \frac{\kappa}{k}}{\alpha_2 F}\right) < U_s < \max\left(-\frac{\beta}{\alpha_1 F}, \frac{\beta + \frac{\kappa}{k}}{\alpha_2 F}\right)$ . It is similar to the results of Chen and Kamenkovich (2013).

*Case two:* In the absence of topography and  $\frac{d^2 U_n}{dy^2} \neq 0$ , the baroclinic instability is determined by the second derivative of quadric shear basic zonal flows, stratification effect and the planetary vorticity gradient  $\beta$ ;

*Case three:* If the gradient of the basic state absolute vorticity  $\beta - \frac{d^2 U_n}{dy^2} \neq 0$ , that is to say, the basic velocity distribution must be such that  $\frac{d^2 U_n}{dy^2}$  is able to over-balance planetary vorticity  $\beta$  to make  $P_n$  change its sign, especially we shall consider the simplest case of the basic zonal flows  $U_n(y) = \overline{U}_n(1 - a_n y^2)$  (where  $\overline{U}_n > 0, 0 < a_n < 1$  are constant). Pedlosky (1987) shows that the absolute vorticity  $\beta - \frac{d^2 U_n}{dy^2} = \beta + 2a_n \overline{U}_n$  must be positively;

*Case four:* When the topography is a east-west topography,  $\frac{\kappa}{k}$  is simplified to  $S_y$ , if the topographic slope  $S_y$  is the southward slope ( $S_y > 0$ ), it can stabilise the basic zonal flow through changing the background PV gradient  $\beta - \frac{d^2 U_2}{dy^2} - \alpha_2 F U_s + S_y$ ; the topographic slope is the northward slope ( $S_y < 0$ ), it is the opposite of the northward slope. When the topography is north-south, it effect on the basic zonal flows through changing  $U_s - \frac{\beta + \frac{\kappa}{k}}{\alpha_2 F}$  in Eq. (16),  $\frac{\kappa}{k}$  is simplified to  $-\frac{l}{k} S_x$  and is dependent of the north-south direction slope, the wavevector magnitude and orientation.

### 3.2. The dispersion relation with the quadric shear basic zonal flows and bottom topography

Nontrivial solutions for  $A_1$  and  $A_2$  of Eqs. (10) and (11) exist only if the determinant of coefficients is zero. This condition yields the dispersion relation

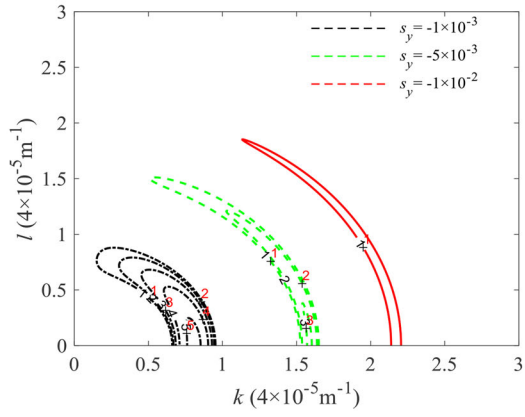
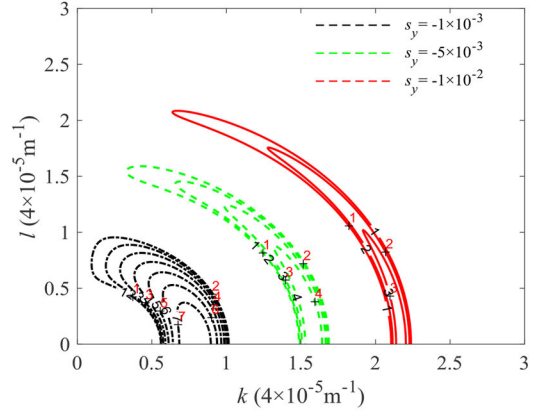
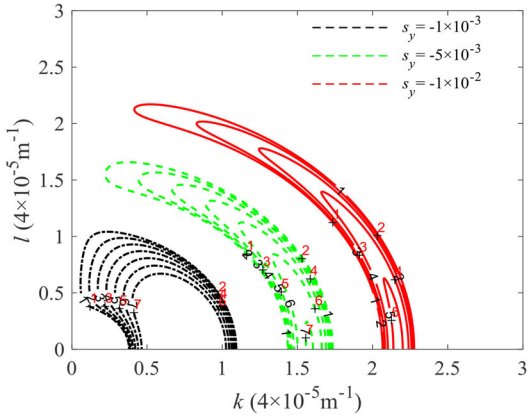
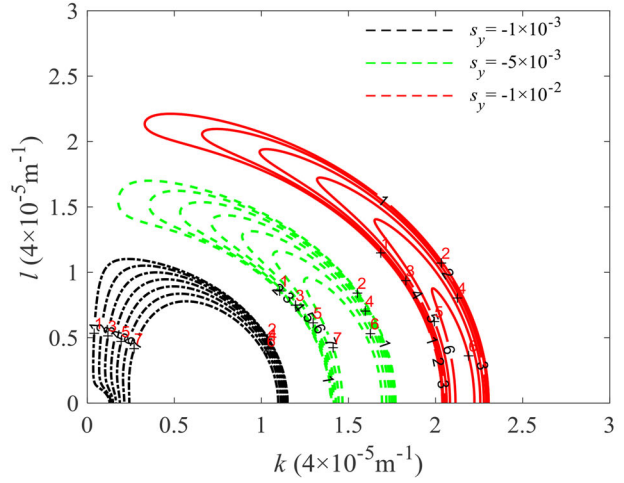
(a)  $U_s = 4 \times 10^2, \frac{d^2 U_1}{dy^2} = 0$ (b)  $U_s = 4 \times 10^{-2}, \frac{d^2 U_1}{dy^2} = -\frac{d^2 U_2}{dy^2} = -1.5 \times 10^{-10}$ (c)  $U_s = 4 \times 10^{-2}, \frac{d^2 U_1}{dy^2} = -\frac{d^2 U_2}{dy^2} = -1 \times 10^{-10}$ (d)  $U_s = 4 \times 10^{-2}, \frac{d^2 U_1}{dy^2} = -\frac{d^2 U_2}{dy^2} = -0.5 \times 10^{-10}$ 

Fig. 1. Spatial structure of unstable modes in the presence of these meridional topographic slopes.

$$\begin{vmatrix} (\omega - U_1 k)(K^2 + \alpha_1 F) + k \left( \beta - \frac{d^2 U_1}{dy^2} + \alpha_1 F U_s \right) & (\omega - U_1 k) \alpha_1 F \\ (\omega - U_2 k) \alpha_2 F & (\omega - U_2 k)(K^2 + \alpha_2 F) + k \left( \beta - \frac{d^2 U_2}{dy^2} - \alpha_2 F U_s \right) + \kappa \end{vmatrix} = 0, \quad (17)$$

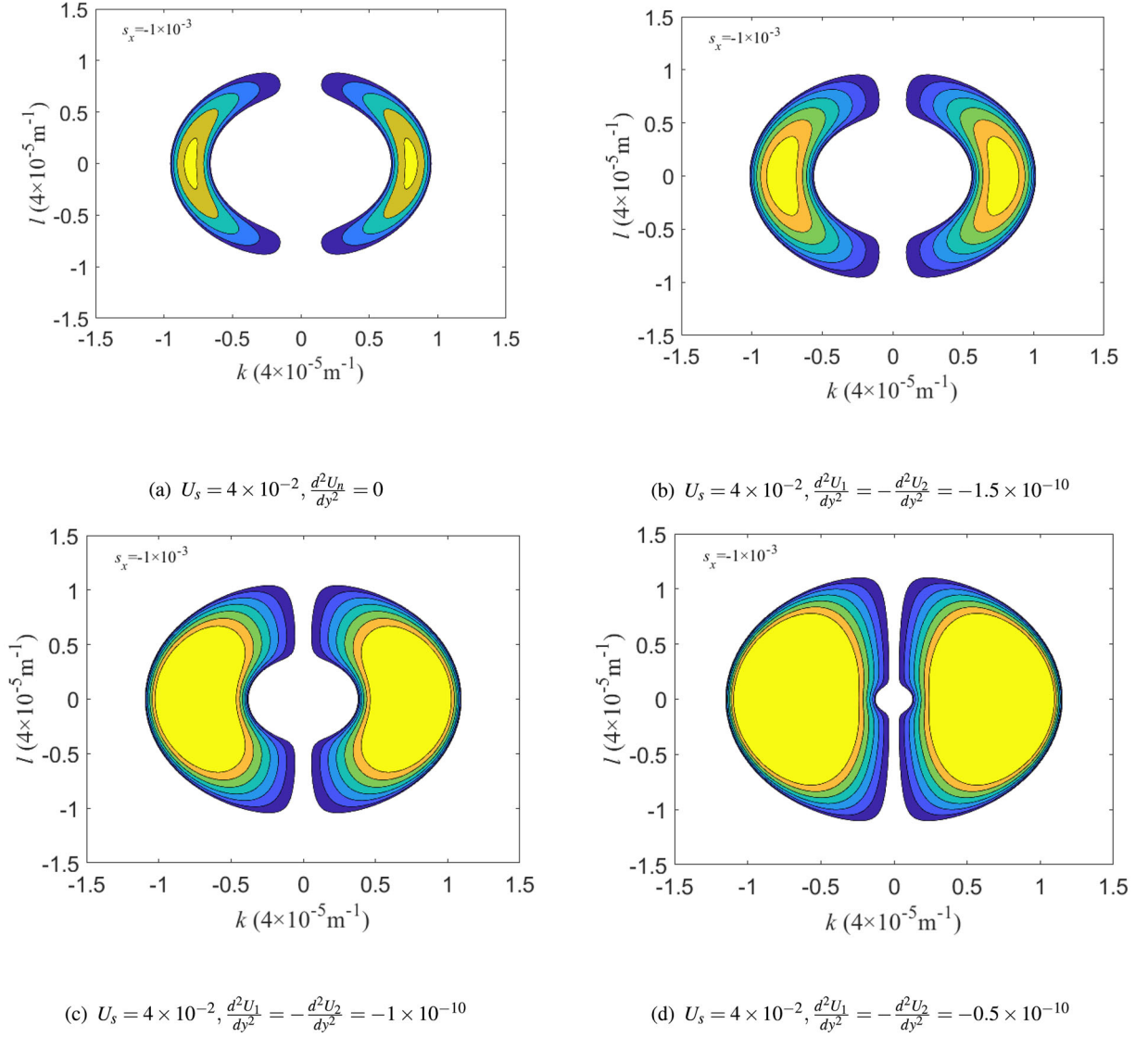


Fig. 2. Spatial structure of unstable modes in the presence of a zonal topographic slope:  $s_x = 1 \times 10^{-3}$ .

Eq. (17) yields a quadratic equation for  $\omega$ ,

$$a\omega^2 + b\omega + c = 0. \quad (18)$$

where

here  $U = U_1 + U_2, S = \frac{\kappa}{k}$ . We can get the phase speed

---


$$\begin{cases} a = K^2(K^2 + F), \\ b = -k \left[ K^2(K^2 + F)U - K^2 \left( 2\beta - \frac{d^2 U_1}{dy^2} - \frac{d^2 U_2}{dy^2} + F(\alpha_1 - \alpha_2)U_s \right) - F \left( \beta - \alpha_2 \frac{d^2 U_1}{dy^2} - \alpha_1 \frac{d^2 U_2}{dy^2} \right) - S(K^2 + \alpha_1 F) \right], \\ c = k^2 \left\{ K^4 U_1 U_2 + K^2 \left( F\alpha_1 U_2^2 + \alpha_2 U_1^2 + U_1 \frac{d^2 U_2}{dy^2} + U_2 \frac{d^2 U_1}{dy^2} - \beta U \right) + \left( \beta - \frac{d^2 U_1}{dy^2} \right) \left( \beta - \frac{d^2 U_2}{dy^2} \right) \right. \\ \left. + F \left[ \beta(\alpha_2 U_1 - \alpha_1 U_2) + \alpha_1 U_2 \frac{d^2 U_2}{dy^2} - \alpha_1 U_1 \frac{d^2 U_2}{dy^2} \right] + \left( \beta - \frac{d^2 U_1}{dy^2} - K^2 U_1 - \alpha_1 F U_2 \right) S \right\}. \end{cases}$$


---

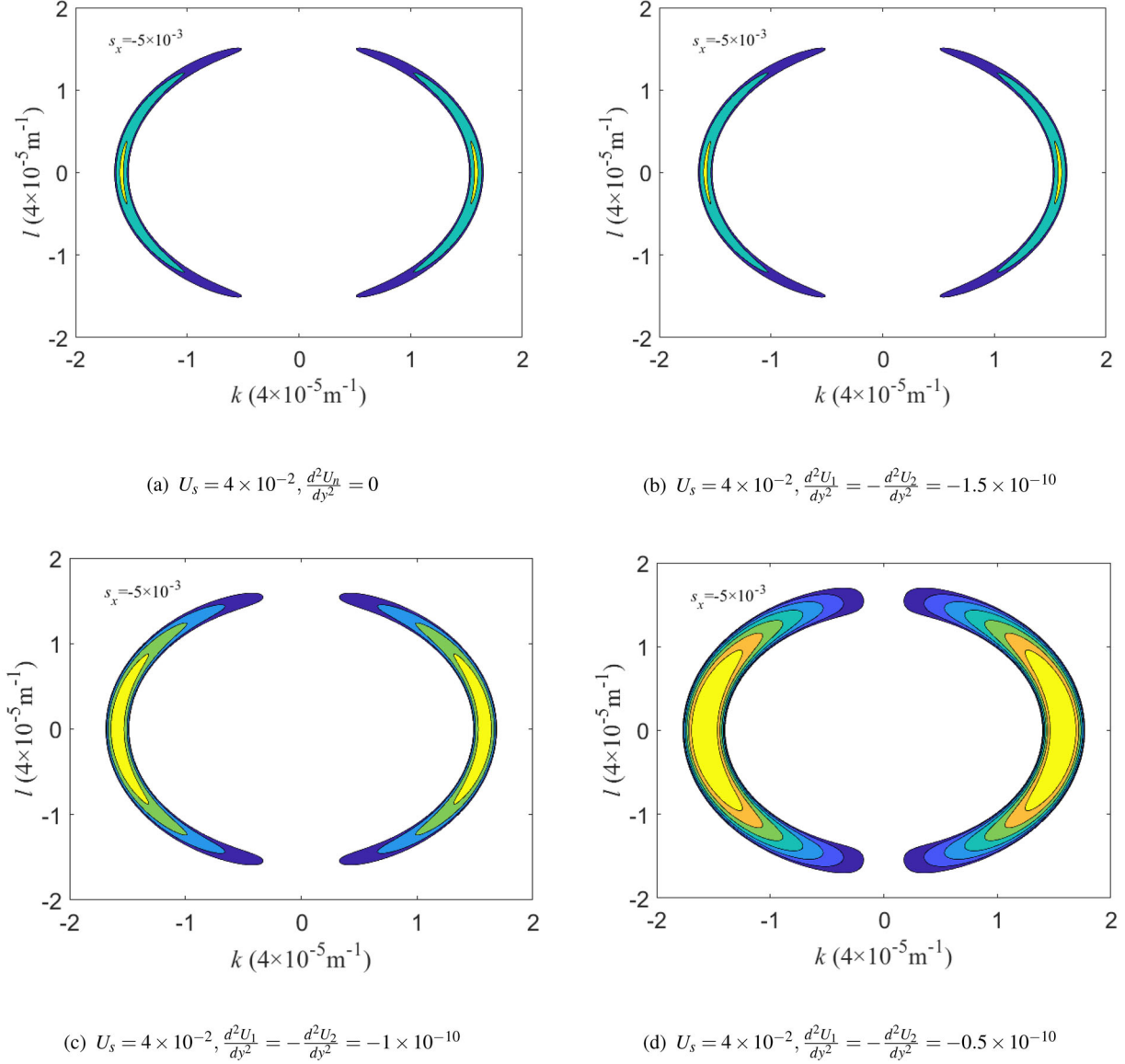


Fig. 3. Spatial structure of unstable modes in the presence of a zonal topographic slope:  $s_x = 5 \times 10^{-3}$ .

and growth rate of unstable wave with the quadric shear basic zonal flows and topographic effects on the  $\beta$  plane approximation, the discriminant of  $\omega$  derived from Eq. (18) is

$$\Delta = b^2 - 4ac, \quad (19)$$

Once  $\Delta < 0$ , the phase speed can be written in a complex form:  $\omega = \omega_r + i\omega_i$ ,  $c = \frac{\omega}{k} = c_r + ic_i$ , where

$$\omega_i = \frac{\sqrt{-\Delta}}{2a}, \quad (20)$$

$$c_r = \frac{-b}{2ak}. \quad (21)$$

The  $c_r$  is a nonlinear function of  $U_n$ ,  $\beta$ ,  $\frac{d^2 U_n}{dy^2}$  and  $S$  for a given perturbation with the wavenumber  $K$ , whilst  $c_i, \omega_i$

are composed of the nonlinear terms. Aside from the terms associated with  $\frac{d^2 U_n}{dy^2}$ , Eqs. (20) and (21) are the same as the results of Chen and Kamenkovich (2013). Using equation (20), we will analyse the effects of the interplay between the second derivative of quadric shear basic zonal flows and topography on the linear baroclinic instability.

3.2.1. Meridional slope and the quadric shear basic zonal flows on the  $\beta$  plane:  $s_x = 0, s_y \neq 0, \frac{d^2 U_n}{dy^2} \neq 0$ . When the slope is only meridional,  $S$  reduces to  $S_y$ . Figure 1a depicts Chen and Kamenkovich's result (2013), Fig. 1b-d shows the growth rate as a function of the wavenumber ( $k, l$ ) and bottom slope for the he quadric shear basic zonal flows:

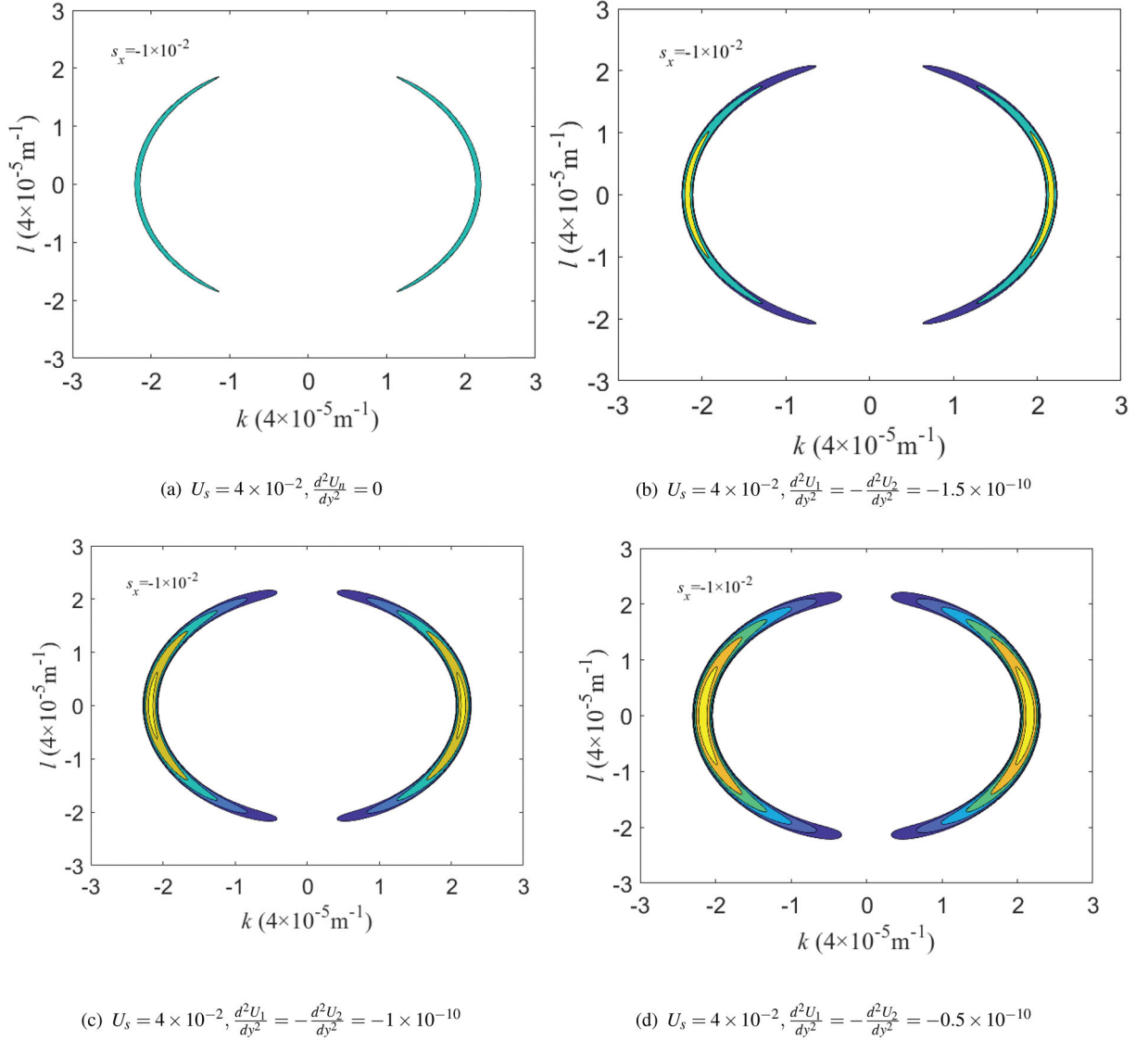


Fig. 4. Spatial structure of unstable modes in the presence of a zonal topographic slope:  $s_x = 1 \times 10^{-2}$ .

$$U_s = U_1 - U_2 = 2U_1 = 4 \times 10^{-2},$$

$$\frac{d^2 U_1}{dy^2} = -1.5 \times 10^{-10}, -1 \times 10^{-10}, -0.5 \times 10^{-10},$$

$$\frac{d^2 U_2}{dy^2} = -\frac{d^2 U_1}{dy^2} = 1.5 \times 10^{-10}, 1 \times 10^{-10}, 0.5 \times 10^{-10}$$

(Geoffrey and Vallis, 2006) over three northward slopes: weak  $-1 \times 10^{-3}$ , intermediate  $-1 \times 10^{-2}$  and strong  $-1 \times 10^{-2}$ . The growth rate of an instability wave depends on the magnitude  $k$ ,  $l$ , topographic slope and the quadric shear basic zonal flows, the instability stable waves are shown here within an incomplete annulus in

the  $(k, l)$  plane. The greatest growth rate is the same as employed in Chen and Kamenkovich (2013) and Leng and Bai (2018), it is found at  $l=0$ , the most instability mode is a meridional noodle mode. Compare Fig. 1a with Fig. 1b-d, as the meridional slope gets steeper, the second derivative of quadric shear basic zonal flows is gradually reduced, the unstable wavenumber rang moves away from the origin in the  $(k, l)$  plane, indication shorter zonal and meridional wavelengths of the unstable modes, and becomes narrower. In addition, Fig. 1b-d shows that the smaller second derivative of quadric shear basic zonal flows can be used to the narrower the width of noodle mode. The results for south slope are also similar and not discussed here.

3.2.2. Zonal slope and the quadric shear basic zonal flows on the  $\beta$  plane:  $s_x \neq 0, s_y = 0, \frac{d^2 U_n}{dy^2} \neq 0$ . Chen and Kamenkovich (2013) has verified that positive (west slope) and negative (east slope) have the same effects on the greatest growth rate and the corresponding phase speed. Thus, we also consider west slope in the following analysis. The effects of a zonal slope are considered for the quadric shear basic zonal flows on slope for the he quadric shear basic zonal flows:  $U_s = U_1 - U_2 = 2U_1 = 4 \times 10^{-2}$ ,  $\frac{d^2 U_1}{dy^2} = -1.5 \times 10^{-10}, -1 \times 10^{-10}, -0.5 \times 10^{-10}$ ,  $\frac{d^2 U_2}{dy^2} = -\frac{d^2 U_1}{dy^2} = 1.5 \times 10^{-10}, 1 \times 10^{-10}, 0.5 \times 10^{-10}$  and the westward slope  $s_x = 1 \times 10^{-3}; 5 \times 10^{-3}; 1 \times 10^{-2}$ . Figures 2a, 3a, 4a and Figs. 2b–d, 3b–d, 4b–d show the basic zonal flows  $U_s = 4 \times 10^{-2}$ ,  $\frac{d^2 U_n}{dy^2} = 0$  and  $\frac{d^2 U_n}{dy^2} \neq 0$  at the different zonal slopes, respectively. Figures 2–4 show that these different zonal topographic slopes are not like a meridional topographic slope on  $\beta$  plane, it modifies the shape of the instability mode, which is no longer the meridional oriented noodle mode, the range model is the circular, and range of instability wavenumber shrinks as slope magnitude increases. Figures 2a, 3a, 4a show the smaller values of the zonal slope correspond to very narrow unstably wavenumber ranges with the same the zonal basic flows  $U_n$ .

In contrast of Figs. 2a, 3a, 4a, as shown in Figs. 2b–d, 3b–d and 4b–d, if the basic zonal flows is the quadric shear basic zonal flows, the effects of  $\frac{d^2 U_n}{dy^2} \neq 0$  are increase the number of unstable wavenumbers areas. But in Figs. 2b–d, 3b–d and 4b–d the range of unstable wavenumbers does not change when  $\frac{d^2 U_n}{dy^2}$  increases, this is totally different from the meridional slope of state.

## 4. Conclusions

The present analysis demonstrates that the bottom topography and the quadric shear basic zonal flows in the baroclinic unstable of oceanic model. We obtained the following conclusions.

(1) Topographic slopes and the quadric shear basic zonal flows are confirmed that it can modify stability of basic zonal flows, through the changes in the background PV gradient on the  $\beta$  plane approximation.

(2) The topographic slope is only meridional slope, the instability mode has the shape of a noodle mode, the width of noodle decreases as the meridional slope (north slope) increases, this illustration that the north slope always plays on unstable role. The function second derivative of quadric shear basic zonal flows ( $\frac{d^2 U_n}{dy^2} \neq 0$ ) are to keep the noodle mode away from  $(k, l)$  plane, when it increase, the width of the mode region become more and more narrow. Therefore, the decrease of  $\frac{d^2 U_n}{dy^2}$  and the steepening of slope have the same effect on the instability.

(3) The topographic slope is purely zonal in  $(k, l)$  plane, if  $\frac{d^2 U_n}{dy^2}$  is zero, namely, the basic zonal is not the quadric shear, the unstable range gradually shrinks as the slope magnitude increases; if the basic zonal flows is the quadric shear ( $\frac{d^2 U_n}{dy^2} \neq 0$ ), the number of instability regions are increased, that is, expand the area of unstable regions. But under the same slope, the change of the quadric shear basic zonal flows does not affect the unstable range.

The results of this idealised study are complementary to the literatures (Chen and Kamenkovich, 2013; Leng and Bai, 2018), it can help to interpret the large-scale waves generation over basic zonal flows sheared and more complex topography in the real ocean and atmosphere. More detailed work including nonzonal basic flows, vertical shear in zonal ocean currents, and theoretical study will be considered.

## Disclosure statement

No potential conflict of interest was reported by the authors.

## Funding

This study was supported by Projects 11362012, 11562014 and 41465002 of the National Natural Science Foundation of China, Project of 2018LH04005 the Natural Science Foundation of Inner Mongolia.

## References

- Benilov, E. S. 2001. Baroclinic instability of two-layer flows over one-dimensional bottom topography. *J. Phys. Oceanogr.* **31**, 2019–2025. doi:10.1175/1520-0485(2001)0312.0.CO;2 doi:10.1175/1520-0485(2001)031<2019:BIOTLF>2.0.CO;2
- Blumsack, S. L. and Gierasch, P. J. 1972. Mars: The effects of topography on baroclinic instability. *J. Atmos. Sci.* **29**, 1081–1089. doi:10.1175/1520-0469(1972)029<1081:MTEOTO>2.0.CO;2
- Chen, C. and Kamenkovich, I. 2013. Effects of topography on baroclinic instability. *J. Phys. Oceanogr.* **43**, 790–804. doi:10.1175/JPO-D-12-0145.1
- Chraney, J. G. 1974. The dynamics of long waves in a baroclinic westerly current. *J. Meteorol.* **4**, 136–162.
- Cushman-Roisin, B. 1986. Frontal geostrophic dynamics. *J. Phys. Oceanogr.* **16**, 132–143. doi:10.1175/1520-0485(1986)016<0132:FGD>2.0.CO;2
- Eady, E. T. 1949. Long waves and cyclone waves. *Tellus* **1**, 33–52.
- Geoffrey, K. and Vallis, 2006. *Atmospheric and Oceanic Fluid Dynamics*. New York: Cambridge University Press, pp. 212–213.



- Hart, J. E. 1975a. Baroclinic instability over a slope. Part I: Linear theory. *J. Phys. Oceanogr.* **5**, 625–633. doi:10.1175/1520-0485(1975)005<0625:BIOASP>2.0.CO;2
- Hart, J. E. 1975b. Baroclinic instability over a slope. Part II: Finite-amplitude theory. *J. Phys. Oceanogr.* **5**, 634–641. doi:10.1175/1520-0485(1975)005<0634:BIOASP>2.0.CO;2
- Leng, H. and Bai, X. 2018. Baroclinic instability of nonzonal flows and bottom slope effects on the propagation of most unstable wave. *J. Phys. Oceanogr.* **48**, 2923–2936. doi:10.1175/JPO-D-18-0087.1
- McWilliams, J. C. 1974. Forced transient flows and small-scale topography. *Geophys. Fluid Dyn.* **6**, 49–79. doi:10.1080/03091927409365787
- Patoine, A. and Warn, T. 1982. The Interaction of long, quasi-stationary baroclinic waves with topography. *J. Atmos. Sci.* **39**, 1018–1025.
- Pedlosky, J. 1978. A nonlinear model of the onset of upwelling. *J. Phys. Oceanogr.* **8**, 178–187. doi:10.1175/1520-0485(1978)008<0178:ANMOTO>2.0.CO;2
- Pedlosky, J. 1981. Resonant topographic waves in barotropic and baroclinic flows. *J. Atmos. Sci.* **38**, 2626–2641. doi:10.1175/1520-0469(1981)038<2626:RTWIBA>2.0.CO;2
- Pedlosky, J. 1987. *Geophysical Fluid Dynamics*. 2nd ed. New York: Springer, 710 pp.
- Pedlosky, J. 2011. The nonlinear downstream development of baroclinic instability. *J. Mar. Res.* **69**, 750–722.
- Pedlosky, J. 2019. The Effect of beta on the downstream development of unstable chaotic baroclinic waves. *J. Phys. Oceanogr.* **49**, 2337–2343. doi:10.1175/JPO-D-19-0097.1
- Phillips, N. A. 1954. Energy transformations and meridional circulations associated with simple baroclinic waves in a two-level quasi-geostrophic model. *Tellus* **6**, 273–286. doi:10.1111/j.2153-3490.1954.tb01123.x
- Rhines, P. B. and Bretherton, F. 1973. Topographic Rossby waves in a rough-bottomed ocean. *J. Fluid Mech.* **61**, 583–607. doi:10.1017/S002211207300087X
- Steinsaltz, D. 1987. Instability of baroclinic waves with bottom slope. *J. Phys. Oceanogr.* **17**, 2343–2350. doi:10.1175/1520-0485(1987)017<2343:IOBWWB>2.0.CO;2